

Generation of strong cylindrical vector pulses via stimulated Brillouin amplification

Zhi-Han Zhu, Peng Chen, Li-Wen Sheng, Yu-Lei Wang, Wei Hu, Yan-Qing Lu, and Wei Gao

Citation: *Appl. Phys. Lett.* **110**, 141104 (2017); doi: 10.1063/1.4979588

View online: <http://dx.doi.org/10.1063/1.4979588>

View Table of Contents: <http://aip.scitation.org/toc/apl/110/14>

Published by the [American Institute of Physics](#)



Get the scoop on
science funding & policy

Free sign-up
for FYI emails
AIP American Institute of Physics

FYI is an authoritative news and resource center for federal science policy, with a focus on the physical sciences.

Generation of strong cylindrical vector pulses via stimulated Brillouin amplification

Zhi-Han Zhu,^{1,a),b)} Peng Chen,^{2,a)} Li-Wen Sheng,³ Yu-Lei Wang,³ Wei Hu,^{2,c)} Yan-Qing Lu,² and Wei Gao¹

¹Da-Heng Collaborative Innovation Center for Science of Quantum Manipulation and Control, Harbin University of Science and Technology, Harbin 150080, China

²National Laboratory of Solid State Microstructures, Collaborative Innovation Center of Advanced Microstructures and College of Engineering and Applied Sciences, Nanjing University, Nanjing 210093, China

³National Key Laboratory of Science and Technology on Tunable Laser, Harbin Institute of Technology, Harbin 150001, China

(Received 30 December 2016; accepted 21 March 2017; published online 3 April 2017)

Light with transverse polarization structures, such as radial and azimuthal polarization, enables and revives lots of applications based on a light-matter interaction due to its unique focal properties. To date, studies referring to this topic mainly concentrate on a weak-light domain, yet it should have gained more attention in a high-energy domain. Here, we demonstrate the generation of strong single-longitudinal-mode (SLM) cylindrical vector (CV) short pulses via stimulated Brillouin amplification. As a proof-of-principle work, the energy is transferred from a pair of 700 ps pumps to a 300 ps Stokes pulse via parametrically exciting coherent phonons in fluorocarbon liquid. After amplification, a 100 mJ-level SLM CV pulse light with 300 ps duration is obtained. Meanwhile, the phase and polarization structures are high fidelity maintained. This result provides a practicable way to generate strong CV light, and by further extending this mechanism into the beam combination system, even an ultra-high intensity CV light can be expected. *Published by AIP Publishing.* [<http://dx.doi.org/10.1063/1.4979588>]

Science of structured light—the generation and application of light fields with custom transverse intensity, phase, and polarization profiles—has gained enormous progress and gradually become the hottest topic of the optical community over the past decade.^{1,2} In this new subject of modern optics, orbital angular momentum (OAM) plays a crucial role,³ which is associated with light's twisted phase profile. Particularly, the infinite dimensional space spanned by this degree-of-freedom (DOF) has directly given rise to a promising research direction—informatics, ranging from high-capacity optical communications,⁴ high-precise optical metrology,⁵ high-dimension quantum information,^{6–11} to fundamental study for nonlinear optics and quantum theory.^{12–15} In addition to the intensity and phase, the polarization of light can also exhibit a non-uniform transverse distribution once the OAM and spin angular momentum (SAM) DOFs are entangled.¹⁶ Among them, radially polarized light and azimuthally polarized light, two specific members of the so-called cylindrical vector (CV) beam, have received more attention, because their focal regions manifest strong longitudinal electric and magnetic fields, respectively.¹⁷ This striking focal property, such as allowing smaller focal spot, inspires another fascinating research direction of the structured photonics—light-matter interaction, including measurement, imaging, microscopy, and optical manipulation at the nanoscale.^{18–20} In this domain, pulsed light with a single longitudinal mode (SLM) is desirable for

many applications, especially for high-energy applications that expect the ability of shaping the focal property more. For instance, employing CV light may reduce the system size of laser drivers for inertial confinement fusion and corresponding material testing,²¹ and besides, it has been predicted that a strong vortex laser (10^{18} W/cm²) could be used for high-gradient positron acceleration.²² However, in the current stage, it is still a challenge for directly converting strong laser pulses via CV polarization converters, such as spin-orbital coupling based q-plates and metasurfaces,^{23–25} whose damage thresholds are low and particularly for SLM light (i.e., all photons in one quantum state mean a larger complex amplitude).

An alternative method to generate high-power CV pulses is employing a light amplification technique that initiates from a weak seed, such as laser amplification (LA), optical parametric chirped pulse amplification (OPCPA), and energy transfer via stimulated Raman or Brillouin scattering (SRS and SBS).^{26–29} For SLM pulses with a sub-nanosecond duration, the efficiency of LA is lower, while OPCPA needs a specific pump source and larger aperture (the damage threshold of compressor gratings is only a few hundred mJ/cm²), making the whole system complicated. In contrast, amplifying light pulses via SRS and SBS in gases, liquids, and plasmas has many superiorities. For example, liquid and gas media provide much higher damage threshold, and plasmas possess almost a damage-free feature that has been used in the cross-beam energy transfer scheme at the National Ignition Facility.³⁰ So far, amplifications of OAM light via SRS and SBS have been proved.^{31–33} Here, we further demonstrate that SBS can also work for CV light, and in this

^{a)}Z.-H. Zhu and P. Chen contributed equally to this work.

^{b)}Electronic mail: zhuzhihan@hrbust.edu.cn.

^{c)}Electronic mail: huwei@nju.edu.cn.

proof-of-principle experiment, strong SLM CV short pulses are generated via stimulated Brillouin amplification (SBA) in fluorocarbon liquid.

The high-energy SLM picosecond source is provided by a SBS compression Nd:YAG laser system (for details, see Fig. S1 in the [supplementary material](#)). The core of this system is a diode pumped Q-switched nanosecond pulse generator, and the SLM selection property is achieved by employing the geometry layout of the output mirror and an optical flat, a more cost-efficient and simple way compared to the Fabry-Perrot etalon. Then, the pulse is directed to a double-pass laser amplifier with a SBS based phase-conjugation mirror. After the amplification and SBS compression, the final output is 250 mJ SLM pulses with 700 ps duration and 3 mm diameter. The partial of this output is directed and focused into a SBS cell to generate 300 ps Stokes frequency shift seed pulses required for the next step. Here, we focus on the radial CV light that can be expressed as a superposition of two Laguerre-Gaussian (LG) modes with opposite topological charges and circular polarizations, i.e., $(|L, -LG_{01}\rangle + |R, +LG_{01}\rangle)/\sqrt{2}$, or two Hermite-Gaussian (HG) modes in orthogonally linear polarizations, i.e., $(|H, HG_{10}\rangle + |V, HG_{01}\rangle)/\sqrt{2}$.¹⁶ To amplify this CV light via SBA, evidently, a pair of linearly (H+V) or circularly (L+R) polarized pumps with the same energy and phase-matching condition are necessary.

Figure 1 shows the schematic illustration of this proof-of-principle experiment. A non-collinear SBA layout is adopted and the cross angle θ between the two pumps is set as $\theta = 6^\circ$, providing the enough interaction length and acceptable phase-matching condition.^{32,34} The CV seeds are converted from a linearly polarized SLM pulse with 300 ps duration by passing through a q-plate with $q = 0.5$, and the highest energy of the seed pulse is set as 20 mJ, an affordable power for liquid-crystal based spin-orbital devices at 1064 nm. Then, except for the difference in polarization, two identical pump pulses with 700 ps duration interact with the seed pulse in a 10-cm-length coupling cell (CS) containing FC-72 (Brillouin gain: 6 GW/cm^2 ; absorption coefficient $< 10^{-5} \text{ cm}^{-1}$), which is widely used in the SBS compression laser system. Two quarter-wave plates (QWPs) inserted in pump paths are used for converting pump light into required polarization combination (H+V or L+R). After the amplification, the high-energy

output pulses are analyzed by polarization tomography consisting of two wave plates and a polarized beam splitter (PBS). The transverse profiles and energies of output pulses before and after the polarization tomography are recorded by a CCD and an energy meter, respectively.

The configuration of SBA for radial CV light shown in Fig. 1 can be regarded as two mutually independent photon-phonon coupling processes, or rather two pumps, respectively, amplifying corresponding polarization components of the seed. One may point out that amplifying CV light via only one photon-phonon coupling could be achieved by using a CV pump; nevertheless, this assumption neglects a fact that generation of high power CV pumps was actually a bottleneck. The phase-matching condition for a non-collinear SBA used here can be expressed as $\mathbf{q}(\Omega') = \mathbf{k}(\omega_p) - \mathbf{k}(\omega_s)$, where $\mathbf{k}(\omega)$ and $\mathbf{q}(\Omega')$ are the optical and acoustic dispersion relations, respectively, and $\Omega' = \cos(\theta/2)(\omega_p - \omega_s)$ is phonons' frequency generated under this configuration. For such a small cross angle ($\theta = 6^\circ$), $\Omega' \approx \Omega = \omega_p - \omega_s$ (1.1 GHz for FC-72) and considering that the linewidth of the utilized sub-nps pulses is large, the decrease in the coupling efficiency induced by the phase-mismatching is negligible. Besides, compared to all-light based OPA, a major defect of parametric amplification via the light-matter interaction is the noise arising from the interactions between optical fields and non-coherent collective excitations. However, the non-collinear SBA scheme directly avoids this thorny problem, owing to a cross angle existing between the propagation directions of the output signals and the noise.

In our experiment, the seed energy is set as 5 mJ, 10 mJ, and 20 mJ, respectively, and the energy of the two pumps is set from 10 mJ to 100 mJ synchronously with a step of 10 mJ. Figure 2(a) shows the dependence of the output energy upon the input one-way pump energy. The results indicate that total output energy increases linearly with the increase in the input pump energy and a stronger seed can extract more energy from pumps in the same condition. The embedded inset in the top left of Fig. 2(a) shows the average final output energy when the input pump energy is $100 \text{ mJ} \times 2$. We can see that 100 mJ-level SLM CV pulses with 300 ps duration are obtained when inputting a seed pulse of $\sim 20 \text{ mJ}$, corresponding to an approximate 4.6 GW/cm^2 power density (unfocused). In addition, it can be noted that the energy in

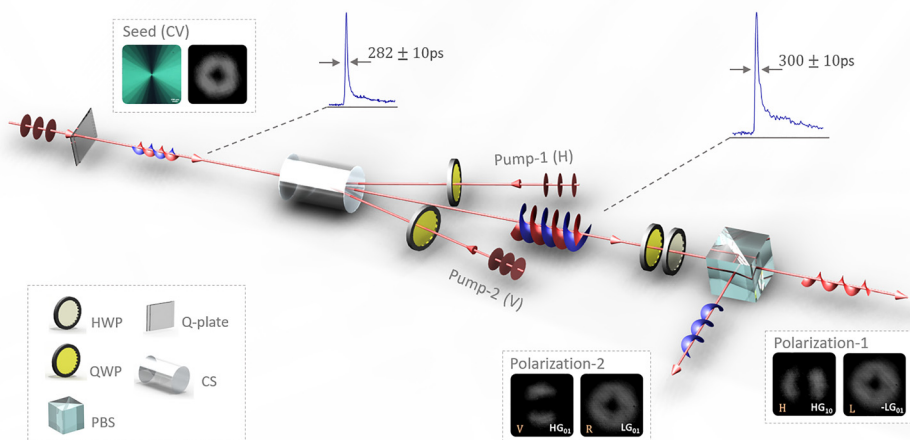


FIG. 1. Schematic illustration of the experimental setup. Key components include the q-plate, half-wave plate (HWP), quarter-wave plate (QWP), polarized beam splitter (PBS), and coupling cell (CS). A CV SLM pulse light with 300 ps duration and Stokes-frequency shift interacts with pump-1 and pump-2 in the coupling cell simultaneously. The polarizations of the two pumps are perpendicular to each other, and the cross angles between them are 6° . Two wave plates and a PBS shown at lower right-hand constitute a polarization tomography module that analyzes energies and transverse profiles of the output signals.

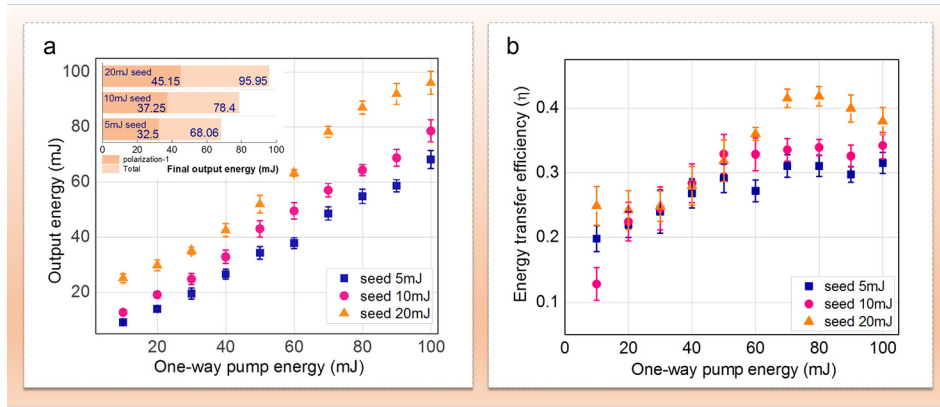


FIG. 2. (a) The output energy of amplified seed pulses versus input one-way pump energy. The top left inset shows the final output energy when the input pump energy is 100 mJ, including total energy and energy in polarization-1. (b) The energy transfer efficiency (η) from pump to Stokes versus the pump energy. The blue, pink, and orange points shown in (a) and (b) correspond to 5 mJ, 10 mJ, and 20 mJ input seed energy, respectively.

polarization-1 is slightly smaller than that in polarization-2. This phenomenon ascribes to an energy difference between the two pumps, and a finer design upon demand can solve this problem. Figure 2(b) shows the energy transfer efficiency (η) from pump to Stokes for different pump energies. As expected, in the same input pump energy, a higher energy ratio of the seed to pump (E_s/E_p) can obtain a higher η .

Moreover, η increases with pump energy for the same seed condition and η becomes saturated as the pump energy reaches 70 mJ. Although η is only achieved up to 40% level under this proof-of-principle configuration, it can be improved rapidly by introducing another group of pumps in the next amplification stage, i.e., so-called SBS beam combination, due to the increase of E_s/E_p . Usually, η can exceed 80% when

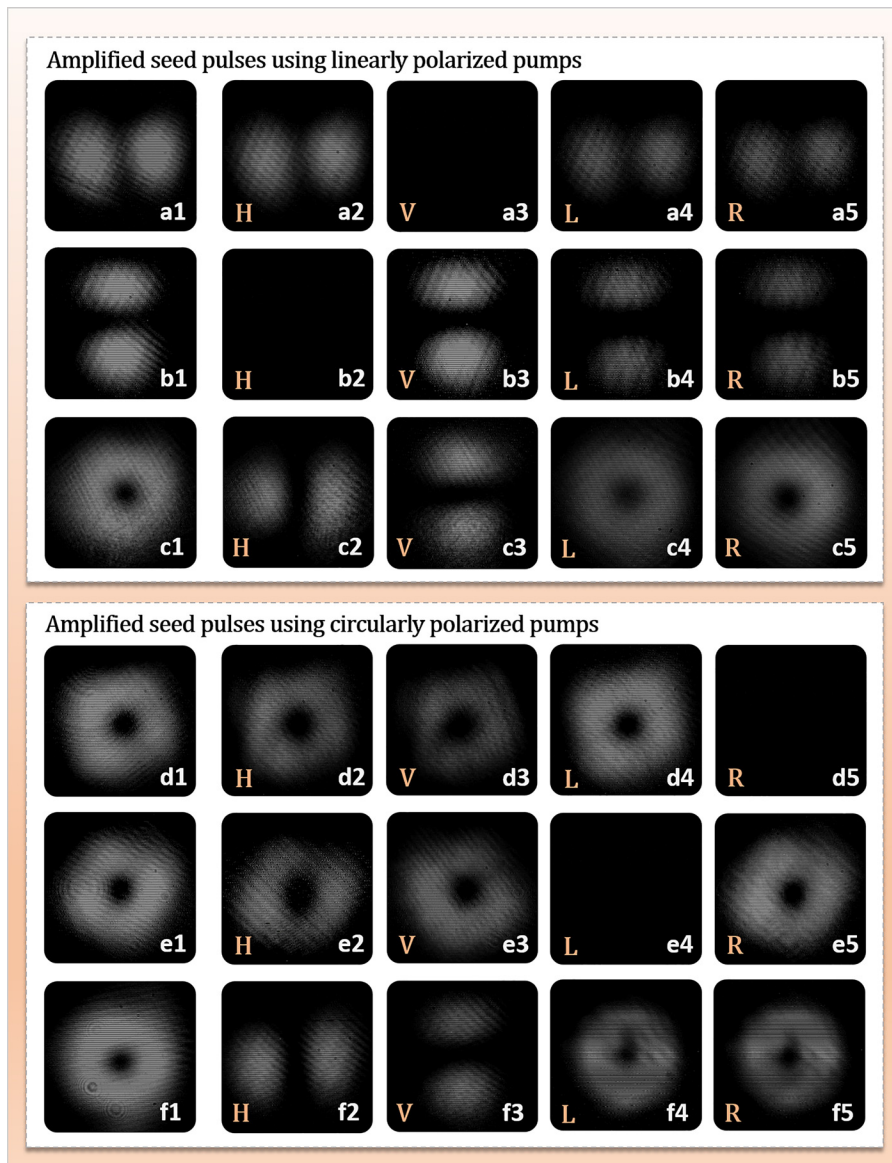


FIG. 3. Transverse profiles and polarization tomographies of the final output pulses; all data are captured with an integration time of 5 s (cumulative exposure of 5 pulses). (a)–(c) The seed is amplified by linearly polarized pumps, (a1)–(a5) only input H polarized pump; (b1)–(b5) only input V polarized pump; (c1)–(c5) both H and V pumps are input. (d)–(f) The seed is amplified by circularly polarized pumps, (d1)–(d5) only input L polarized pump; (e1)–(e5) only input R polarized pump; (f1)–(f5) both L and R pumps are input.

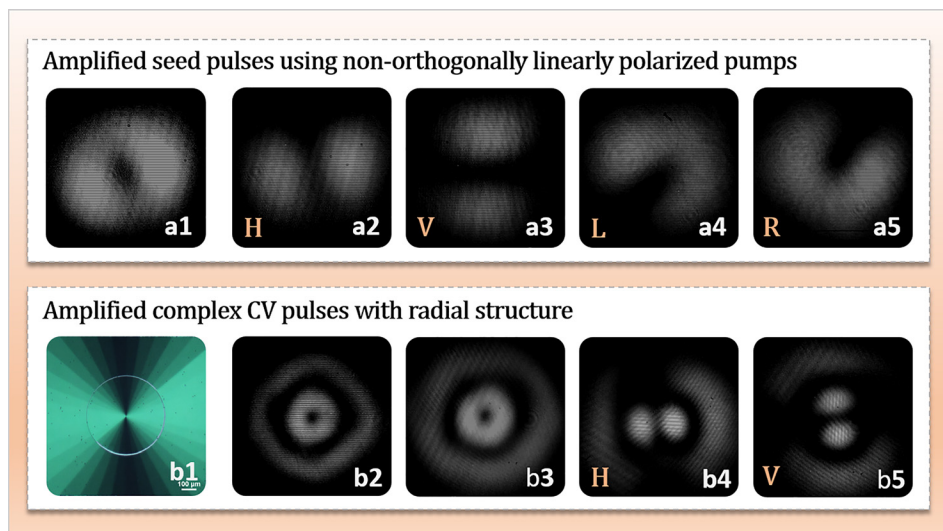


FIG. 4. (a) Transverse profiles and polarization tomography of the final output pulses amplified by two non-orthogonal linearly polarized pumps; all data are captured with 5 s integration time (cumulative exposure of 5 pulses). (b1) Micrograph of a q-plate with $q = 0.5$ and $p = 1$, (b2) Transverse profile of the input complex CV pulses, and (b3)–(b5) Transverse profiles and polarization tomography of the final output complex CV pulses.

E_s/E_p is greater than 4 in the FC-72 based SBA system in the high energy range,³⁵ providing a feasible way to generate ultra-high intensity CV pulses.

Data shown in Fig. 2 involve two cases, H+V and L+R pumps. As expected, there is no difference reflected in the output energy between adopting orthogonally linear polarizations and opposite circular polarizations. This situation is also proved by measuring transverse profiles, with the polarization tomographies of the final output pulses with 100 mJ pumped shown in Fig. 3. It can be seen that the output pulses seem to be a HG or LG mode under one-way pump, as shown in Figs. 3(a), 3(b), 3(d), and 3(e). This is because that after the amplification, only pump-1 input, the original seed field evolves into $\alpha|L, -LG_{01}\rangle + \beta|R, +LG_{01}\rangle$ or $\alpha|H, HG_{10}\rangle + \beta|V, HG_{01}\rangle$ where $|\alpha|^2 + |\beta|^2 = 1$ and $\alpha : \beta \approx 5 : 1$. Thus, comparing the amplified component with unamplified component, the latter becomes too weak at the same attenuation level. Once the two pumps input simultaneously, as shown in Figs. 3(c) and 3(f), the output pulses manifest a typical characteristic of radial CV light indicated by corresponding polarization tomography.

Notice that in order to achieve a high fidelity amplification, a key point is the orthogonality between the two pumps, or the output light field's structure in polarization and spatial DOF will distort. For instance, as shown in Fig. 4(a), after an amplification was performed by two non-orthogonal linearly polarized pumps, the donut transverse profile becomes non-uniform and its polarization tomography in L and R projection even manifests LG modes with fractal topological charges. In addition to the standard radial and azimuthal pulses, SBA can also be applied for amplifying more complex CV light.^{25,36,37} Figure 4(b) shows the polarization tomography of amplified CV pulses with a radial structure. By employing such high-energy SLM complex CV pulses, a more flexible focal property can be provided for the research on the light-matter interaction.

In summary, we have demonstrated the generation of high-energy SLM CV short pulses via SBA, and a 100 mJ-level radial CV light with 300 ps pulse duration is achieved. After the amplification, measurements of polarization tomography in energy and transverse profile indicate that the polarization structures are maintained with high fidelity.

These results suggest that the SBA is a feasible way to generate high power CV light, and ultra-high intensity CV pulses could be generated by further extending this configuration into a multi-pumped beam combination system. What's more, this mechanism can also work in plasma based SBS systems, to generate ultra-high energy CV fs pulses.

See [supplementary material](#) for the optical layout of the high-energy SLM picosecond source.

This work was supported by the National Natural Science Foundation of China (Grant Nos. 61378003, 61490714, 61575093, and 11574065) and the Key Programs of the Natural Science Foundation of Heilongjiang Province of China (Grant No. ZD201415).

¹A. M. Yao and M. J. Padgett, *Adv. Opt. Photonics* **3**, 161 (2011).

²J. P. Torres and L. Torner, *Twisted Photons: Applications of Light with Orbital Angular Momentum* (John Wiley & Sons, 2011).

³L. Allen, M. W. Beijersbergen, R. J. C. Spreeuw, and J. P. Woerdman, *Phys. Rev. A* **45**, 8185 (1992).

⁴J. Wang, J. Yang, I. M. Fazal, N. Ahmed, Y. Yan, H. Huang, Y. Ren, Y. Yue, S. Dolinar, M. Tur, and A. E. Willner, *Nat. Photonics* **6**, 488 (2012).

⁵V. D'Ambrosio, N. Spagnolo, L. Del Re, S. Sulssarenko, Y. Li, L. C. Kwek, L. Marrucci, S. P. Walborn, L. Aolita, and F. Sciarrino, *Nat. Commun.* **3**, 961 (2012).

⁶X. Wang, X. Cai, Z. Su, M. Chen, D. Wu, L. Li, N. Liu, C. Lu, and J. Pan, *Nature* **518**, 516 (2015).

⁷G. Molina-Terriza, J. P. Torres, and L. Torner, *Phys. Rev. Lett.* **88**, 013601 (2001).

⁸R. Fickler, R. Lapkiewicz, W. N. Plick, M. Krenn, C. Schaeff, S. Ramelow, and A. Zeilinger, *Science* **338**, 640 (2012).

⁹D.-S. Ding, W. Zhang, Z.-Y. Zhou, S. Shi, G.-Y. Xiang, X.-S. Wang, Y.-K. Jiang, B.-S. Shi, and G.-C. Guo, *Phys. Rev. Lett.* **114**, 050502 (2015).

¹⁰Z. Y. Zhou, S. L. Liu, Y. Li, D. S. Ding, W. Zhang, S. Shi, B. S. Shi, and G. C. Guo, *Phys. Rev. Lett.* **117**, 103601 (2016).

¹¹A. Nicolas, L. Veissier, L. Giner, E. Giacobino, D. Maxein, and J. Laurat, *Nat. Photonics* **8**, 234 (2014).

¹²Z.-Y. Zhou, D.-S. Ding, Y.-K. Jiang, Y. Li, S. Shi, X.-S. Wang, and B.-S. Shi, *Opt. Express* **22**, 20298 (2014).

¹³Z. Zhu, W. Gao, C. Mu, and H. Li, *Optica* **3**, 212 (2016).

¹⁴Z. H. Zhu, L. W. Sheng, Z. W. Lv, W. M. He, and W. Gao, *Sci. Rep.* **7**, 40526 (2017).

¹⁵Z.-Y. Zhou, Z.-H. Zhu, S.-L. Liu, Y.-H. Li, S. Shi, D.-S. Ding, L.-X. Chen, W. Gao, G.-C. Guo, and B.-S. Shi, preprint [arXiv:1701.04081](#) (2017).

- ¹⁶F. Cardano, E. Karimi, S. Slussarenko, L. Marrucci, C. D. Lisio, and E. Santamato, *Appl. Opt.* **51**, C1 (2012).
- ¹⁷R. Dorn, S. Quabis, and G. Leuchs, *Phys. Rev. Lett.* **91**, 233901 (2003).
- ¹⁸Q. Zhan, *Adv. Opt. Photonics* **1**, 1 (2009).
- ¹⁹L. Yan, P. Gregg, E. Karimi, A. Rubano, L. Marrucci, R. Boyd, and S. Ramachandran, *Optica* **2**, 900 (2015).
- ²⁰T. Bauer, P. Banzer, E. Karimi, S. Orlov, A. Rubano, L. Marrucci, E. Santamato, R. W. Boyd, and G. Leuchs, *Science* **347**, 964 (2015).
- ²¹R. Betti, C. D. Zhou, K. S. Anderson, L. J. Perkins, W. Theobald, and A. A. Solodov, *Phys. Rev. Lett.* **98**, 155001 (2007).
- ²²J. Vieira and J. T. Mendonca, *Phys. Rev. Lett.* **112**, 215001 (2014).
- ²³L. Marrucci, C. Manzo, and D. Paparo, *Phys. Rev. Lett.* **96**, 163905 (2006).
- ²⁴F. Bouchard, I. D. Leon, S. A. Schulz, J. Upham, E. Karimi, and R. W. Boyd, *Appl. Phys. Lett.* **105**, 101905 (2014).
- ²⁵W. Ji, C. H. Lee, P. Chen, W. Hu, Y. Ming, L. Zhang, T. H. Lin, V. Chigrinov, and Y. Q. Lu, *Sci. Rep.* **6**, 25528 (2016).
- ²⁶L. Lancia, J. R. Marquès, M. Nakatsutsumi, C. Riconda, S. Weber, S. Hüller, A. Mančić, P. Antici, V. T. Tikhonchuk, A. Héron, P. Audebert, and J. Fuchs, *Phys. Rev. Lett.* **104**, 025001 (2010).
- ²⁷S. Weber, C. Riconda, L. Lancia, J. R. Marquès, G. A. Mourou, and J. Fuchs, *Phys. Rev. Lett.* **111**, 055004 (2013).
- ²⁸M. R. Edwards, N. J. Fisch, and J. M. Mikhailova, *Phys. Rev. Lett.* **116**, 015004 (2016).
- ²⁹L. Lancia, A. Giribono, L. Vassura, M. Chiaramello, C. Riconda, S. Weber, A. Castan, A. Chatelain, A. Frank, T. Gangolf, M. N. Quinn, J. Fuchs, and J. R. Marquès, *Phys. Rev. Lett.* **116**, 075001 (2016).
- ³⁰J. D. Moody, P. Michel, L. Divol, R. L. Berger, E. Bond, D. K. Bradley, D. A. Callahan, E. L. Dewald, S. Dixit, M. J. Edwards, S. Glenn, A. Hamza, C. Haynam, D. E. Hinkel, N. Izumi, O. Jones, J. D. Kilkenny, R. K. Kirkwood, J. L. Kline, W. L. Kruer, G. A. Kyrala, O. L. Landen, S. LePape, J. D. Lindl, B. J. MacGowan, N. B. Meezan, A. Nikroo, M. D. Rosen, M. B. Schneider, D. J. Strozzi, L. J. Suter, C. A. Thomas, R. P. J. Town, K. Widmann, E. A. Williams, L. J. Atherton, S. H. Glenzer, and E. I. Moses, *Nat. Phys.* **8**, 344 (2012).
- ³¹J. T. Mendonça, B. Thidé, and H. Then, *Phys. Rev. Lett.* **102**, 185005 (2009).
- ³²W. Gao, C. Mu, H. Li, Y. Yang, and Z. Zhu, *Appl. Phys. Lett.* **107**, 041119 (2015).
- ³³J. Vieira, R. M. G. M. Trines, E. P. Alves, R. A. Fonseca, J. T. Mendonça, R. Bingham, P. Norreys, and L. O. Silva, *Nat. Commun.* **7**, 10371 (2016).
- ³⁴Y. Chen, Z. Lu, Y. Wang, and W. He, *Opt. Lett.* **39**, 3047 (2014).
- ³⁵Q. Guo, Z. Lu, and Y. Wang, *Appl. Phys. Lett.* **96**, 221107 (2010).
- ³⁶P. Chen, W. Ji, B. Y. Wei, W. Hu, V. Chigrinov, and Y. Q. Lu, *Appl. Phys. Lett.* **107**, 241102 (2015).
- ³⁷P. Chen, S. J. Ge, L. L. Ma, W. Hu, V. Chigrinov, and Y. Q. Lu, *Phys. Rev. Appl.* **5**, 044009 (2016).